

1. Introduction

The Ni-base alloys used as construction material in light water reactors (LWRs) have experienced stress corrosion cracking (SCC). Primary-water SCC of Alloy 600 steam generator tubes in pressurized water reactors (PWRs) has been studied intensively.¹⁻³ Stress corrosion cracking has also occurred in Ni alloys used in applications such as instrument nozzles and heater thermal sleeves in the pressurizer⁴ and penetrations for the control-rod drive mechanism (CRDM) in the reactor vessel closure heads.⁵ In the fall of 1991, during an over-pressurization test, a leak was discovered in the pressure-vessel head penetration at the Bugey 3 plant in France. Metallurgical evaluations indicated that the leak was caused by primary-water SCC.⁶ The main crack had initiated in Alloy 600 base metal and propagated into the Alloy 182 weld metal. Subsequent inspections of CRDM penetrations in domestic and foreign PWRs identified a small number of penetrations (<5% of the penetrations inspected) with axial cracks. None of the cracks was through-wall, and until recently, no more leaks occurred in pressure-vessel head penetrations.

Leaks from axial through-wall cracks were identified at Oconee unit 1 in November 2000 and at Arkansas Nuclear One unit 1 in February 2001.⁷ During the next 15 months, inspections at Oconee units 2 and 3 and followup inspection at unit 1 identified both axial and circumferential cracks in reactor-vessel head penetrations.⁸ The presence of circumferential cracks, in particular, raised concerns regarding structural integrity.^{9,10} Also, in October 2000, significant boron deposits were discovered near the Loop "A" reactor vessel nozzle to hot-leg reactor coolant pipe weld at the V. C. Summer plant.¹¹ Ultrasonic inspection of the pipe revealed an axial crack and a short, intersecting circumferential crack, in the dissimilar metal weld at the top of the pipe. Earlier in 2000, two shallow axial flaws were found in the outlet nozzle-to-safe-end weld of Ringhals unit 3, and four axial indications were found in the same region of Ringhals unit 4, in Sweden.¹² Cracks have also been found in pressure-vessel head penetrations at North Anna unit 2,¹³ the Davis-Besse nuclear power plant,¹⁴ and more recently, in the bottom-mounted instrumentation nozzles at South Texas unit 1.^{15,16} Long-term operating experience indicates that, although wrought Ni-base Alloy 600 is susceptible to SCC, until recently, the weld metal Alloys 82 and 182 used with Alloy 600 were perceived to be less susceptible. However, laboratory tests indicate that in PWR coolant environments, the SCC susceptibility of Alloy 182 is greater than Alloy 600, and Alloy 82 is comparable to Alloy 600. This apparent inconsistency between field and laboratory experience has been an issue that needs further investigation.

The objective of the experimental program being conducted at Argonne National Laboratory (ANL) is to evaluate the resistance of Ni alloys and their welds to environmentally assisted cracking in simulated LWR coolant environments. The present report is focused on the cracking behavior of laboratory-prepared Alloy 182 welds as a function of loading and sample orientation.

In order to meet the objective, CGR tests on samples of Alloy 182 were conducted in a PWR environment. The approach was to precrack the samples in water and continue with loading cycles with increasing load ratios, R , and increasing rise times. Finally, the samples were set at constant load to determine SCC CGRs. This approach assured a complete SCC engagement and a uniform crack front. Each test was complemented by a detailed fractographic examination. One notes that the ANL approach is different from the commonly used practice in that, at ANL, precracking was conducted in water as opposed to air. One important advantage is that major experimental difficulties such as incomplete intergranular fracture mode engagement and finger-like crack growth were never encountered in our program.

The resulting cyclic crack growth rate (CGR) data in water for Alloy 182 was compared with the CGR in air for Alloy 600 obtained previously to determine the effect of the PWR environment. The effect of key parameters on both cyclic and constant load CGRs were determined previously.¹⁷⁻²¹ As such, correlations describing the fatigue CGRs of Alloys 600 and 690 as a function of the stress intensity factor range ΔK , load ratio R , and temperature were developed.²² The results indicated that in air, the CGRs of these materials are relatively insensitive to changes in the test frequency. The CGR (da/dN in m/cycle) of Alloy 600 in air is best expressed as

$$da/dN = C_{A600} (1 - 0.82 R)^{-2.2} (\Delta K)^{4.1}, \quad (1)$$

where ΔK is in $\text{MPa}\cdot\text{m}^{1/2}$, and constant C_{A600} is given by a third-order polynomial of temperature T ($^{\circ}\text{C}$) expressed as

$$C_{A600} = 4.835 \times 10^{-14} + (1.622 \times 10^{-16})T - (1.490 \times 10^{-18})T^2 + (4.355 \times 10^{-21})T^3. \quad (2)$$

In high-dissolved-oxygen (DO) water, the CGRs of Alloy 600 showed frequency-dependent enhancement under cyclic loading conditions. Nevertheless, in high-DO water, the environmental enhancement of growth rates did not appear to depend strongly on the material condition. In contrast, environmental enhancement of CGRs of Alloy 600 in low-DO water seemed to be strongly dependent on material conditions. In the literature²³⁻²⁷ such variability has been attributed to thermo-mechanically-controlled parameters such as yield strength and grain boundary coverage of carbides, although the evidence for this dependence is more substantial for steam generator tubing than thicker structural materials.

In the earlier ANL work, correlations were also developed to estimate the enhancement of CGRs in LWR environments relative to the CGRs in air under the same loading conditions. The best-fit curve for Alloy 600, either in the solution annealed (SA) condition or the SA plus thermally treated condition, in ≈ 300 ppb DO water is given by the expression¹⁹

$$\text{CGR}_{\text{env}} = \text{CGR}_{\text{air}} + 4.4 \times 10^{-7} (\text{CGR}_{\text{air}})^{0.33}. \quad (3)$$

Experimental results showed that some materials in PWR environments show little enhancement, while others show enhancement at 320°C comparable to that predicted by Eq. 3. The SCC of Alloy 600 has been reviewed by Chopra et al.²² and more recently in Ref. 28, and was found that frequency-dependent environmental enhancement is usually associated with susceptibility to SCC under constant loading conditions.

Finally, the existing SCC CGR data for Ni-alloy weld metals (e.g., Alloys 82, 182, 52, 152, and 132) have been compiled and evaluated to establish the effects of key material, loading, and environmental parameters on CGRs in PWR environments. The CGR data generated at ANL on laboratory-prepared Alloy 182 welds are compared with the existing CGR data for Ni-alloy welds to determine their relative susceptibility to environmentally enhanced cracking under a variety of loading conditions.

2 Experimental

2.1 Material and Specimen Design

Crack growth rate tests have been conducted on Alloy 182 weld metal samples in simulated PWR environments at 320°C in accordance with ASTM Designation E 647, “Standard Test Method for Measurement of Fatigue Crack Growth Rates.” The tests were performed on 1-T compact tension (CT) specimens; configuration of the CT specimen is shown in Fig. 1. Crack extensions were determined by the reversing DC potential drop technique.

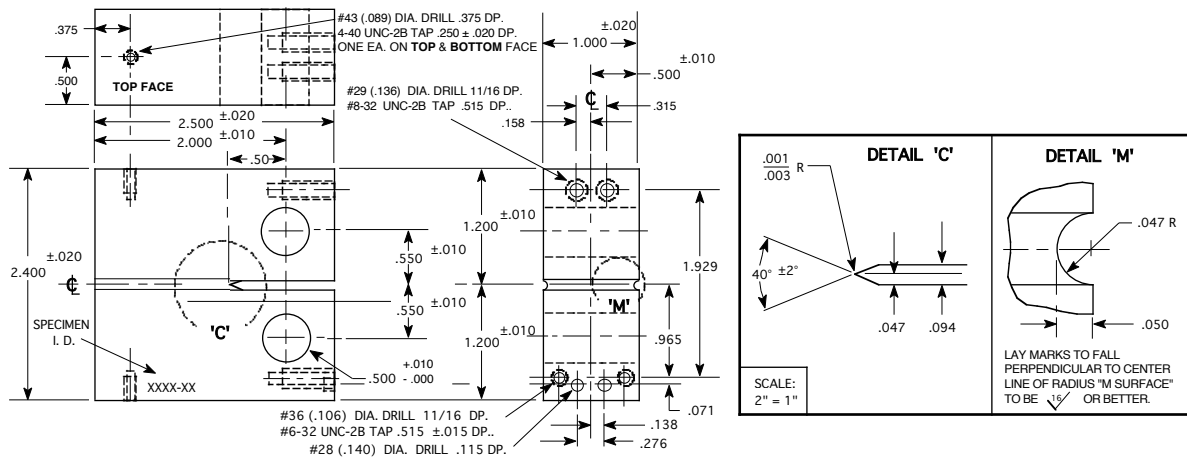


Figure 1. Configuration of compact-tension specimen used for this study (dimensions in inch)

The 1-T CT specimens were machined from laboratory-prepared double-J weld (Fig. 2a) and deep-groove filled weld (Fig. 2b). The double-J weld was prepared by joining two 152 x 305 mm (6 x 12 in.) pieces of 38-mm-thick (1.5-in.-thick) plate (Heat NX1310). It was produced by 48 weld passes, root passes 1–5 involved gas tungsten arc (GTA) welding with Alloy 82 filler/electrode, and the other passes, SMA welding with Alloy 182 filler. A schematic of the weld design and various passes is shown in Fig. 2a, and the conditions for each weld pass are listed in Table 2. During welding the maximum inter-pass temperature was $\approx 120^{\circ}\text{C}$ (250°F), and the weld surfaces were cleaned by wire brushing and grinding and were rinsed with de-mineralized water or alcohol. The deep-groove filled weld was prepared by using a 51-mm thick Alloy 600 plate (Heat NX1933) with a deep groove that was filled by several passes of SMA welding with Alloy 182 filler/electrode (size 1/8 or 5/32 in.) (Fig. 2b). The chemical compositions of the base and weld metals are given in Table 1.

Table 1. Chemical composition (wt.%) of Alloy 600 base metal and Inconel 182 and 82 weld metals.

Alloy ID (Heat)	Analysis	C	Mn	Fe	S	P	Si	Cu	Ni	Cr	Ti	Nb	Co
A 600 (NX1310)	Vendor	0.07	0.22	7.39	0.002	0.006	0.12	0.05	76.00	15.55	0.24	0.07	0.058
	ANL	0.07	0.22	7.73	0.001	–	0.18	0.06	75.34	–	–	–	–
A 600 (NX1933)	Vendor	0.08	0.26	9.55	0.003	–	0.15	0.10	73.31	15.90	–	–	–
	A 182	Spec.	0.10*	5.0–9.5	6.0–10.0	0.015*	–	1.0*	0.5*	Bal	13.0–17.0	1.0*	1.0–2.5
A 182 Double-J	ANL	0.04	6.58	6.48	0.005	0.022	0.33	0.04	70.62	14.34	0.36	1.13	0.03
A 182 Deep Groove	ANL	0.04	7.08	6.82	0.005	0.025	0.35	0.03	70.44	13.81	0.30	1.06	0.02
A 82	Spec.	0.10*	2.5–3.5	3.0*	0.015*	–	0.5*	0.5*	67.00*	18.0–22.0	0.75*	2.0–3.0	0.75*

*Maximum.

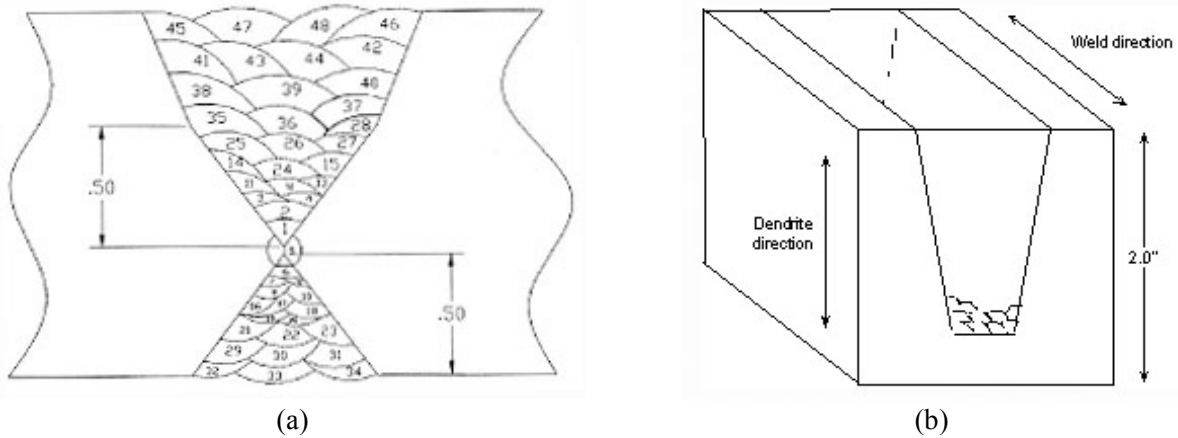


Figure 2. Schematic of the weld joint design and weld passes for (a) Alloy 182 SMA double-J weld and (b) the deep-groove weld (dimensions are in inches).

Table 2. Welding process and conditions for various weld passes.

Weld Pass	Process	Filler Metal	Filler/Electrode Size (in.)	Current (A)	Voltage (V)	Travel Speed (in./min)
1 – 5	GTA	Alloy 82	3/32	185 – 215	21 – 22	2 – 4
6 – 10	SMA	Alloy 182	3/32	140 – 155	24 – 26	6 – 7
11 – 27	SMA	Alloy 182	1/8	155 – 170	25 – 27	6 – 7
28 – 48	SMA	Alloy 182	5/32	170 – 180	26 – 28	6 – 7

Two 1-T CT specimens were cut from the double-J Alloy 182 SMA weld in the TS orientation,* as shown schematically in Fig. 3a. Three additional 1-T CT specimens, in TS, TL and LS orientations, were prepared from a deep-groove Alloy 182 weld (Fig. 3b). All 1-T CT specimens were 25.4-mm (1-in.) thick as shown in Fig. 1, except the deep-groove specimen in LS orientation that had to be thinned to a thickness of 19.4 mm to ensure that the entire crack front would be exclusively in the weld alloy.

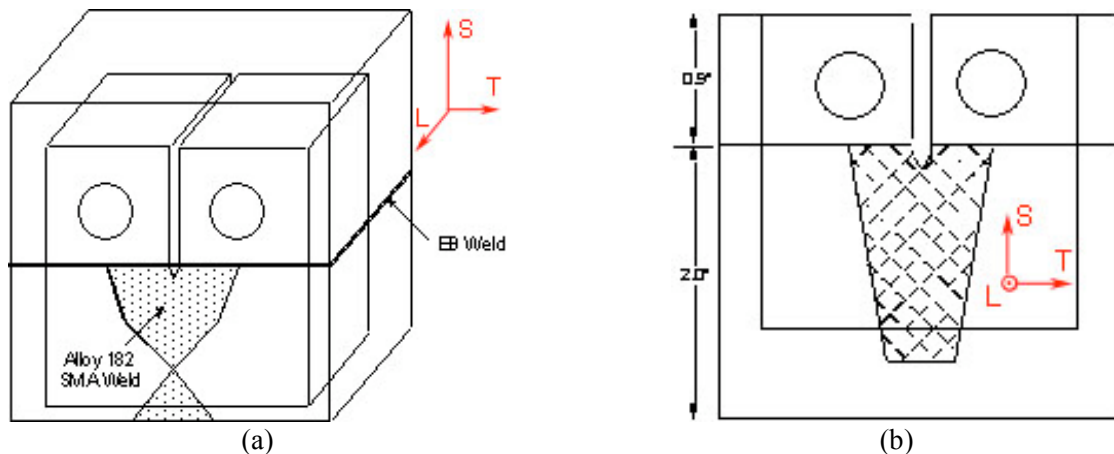


Figure 3. Orientation of the CT specimens from (a) the Alloy 182 SMA double-J weld and (b) the deep-groove weld.

*The first letter represents the direction normal to the fracture plane and the second represents the direction of crack advance. The three directions are: T = transverse, L = longitudinal, and S = side.

2.2 Test Facility

The facility for conducting CGR tests in water at elevated temperature and pressure consists of the following: an MTS closed-loop electro-hydraulic material test system equipped with an extra-high-load frame rated at 89 kN (20,000 lb) maximum and MTS 810 (or equivalent) control console; hydraulic pump; commercial autoclave with a recirculating or once-through water system; temperature control unit; DC potential control console; two computers for elastic unloading compliance and DC potential measurements; and strip chart recorder. The autoclave, mounted within the load frame, has been modified to permit a ≈ 19 -mm (0.75-in.) shaft to load the test specimen through a “Bal-Seal” gland in the top of the autoclave cover. Up to three 25.4-mm (1-in.) thick (1-T) CT specimens can be tested in series inside the autoclave. Figure 4 shows a photograph of the MTS load frame with the autoclave, temperature control unit and strip chart recorder (on the right), MTS 810 control console (on the left), and DC potential control console (above the MTS 810 system). Two such systems were used for this program; the systems differ only slightly in terms of design and materials of construction.



Figure 4. A photograph of the facility for conducting crack growth tests in simulated LWR environments.

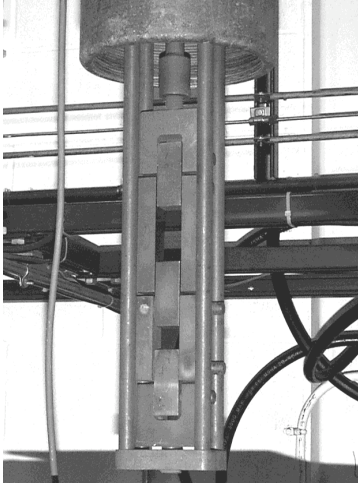


Figure 5.
A photograph of the specimen load train

The test facility is designed for easy access to the specimens during assembly of the test train. The MTS load frame stands ≈ 3.7 m (12 ft) high. The actuator assembly, consisting of the hydraulic actuator, load cell, autoclave plug, and the internal specimen load train, may be raised and lowered hydraulically to position the specimens at a convenient height. A photograph of the specimen load train is shown in Fig. 5. A 1-T CT specimen may be substituted for any or all of the three central in-line blocks.

The autoclave is continuously supplied with the test water solution from a feedwater tank. Figure 6 shows a schematic diagram of the water system. It consists of a feedwater storage tank, high pressure pump, regenerative heat exchanger, autoclave preheater, test autoclave, electrochemical potential (ECP) cell, regenerative heat exchanger, back-pressure regulator, and return line to the feedwater tank. In the

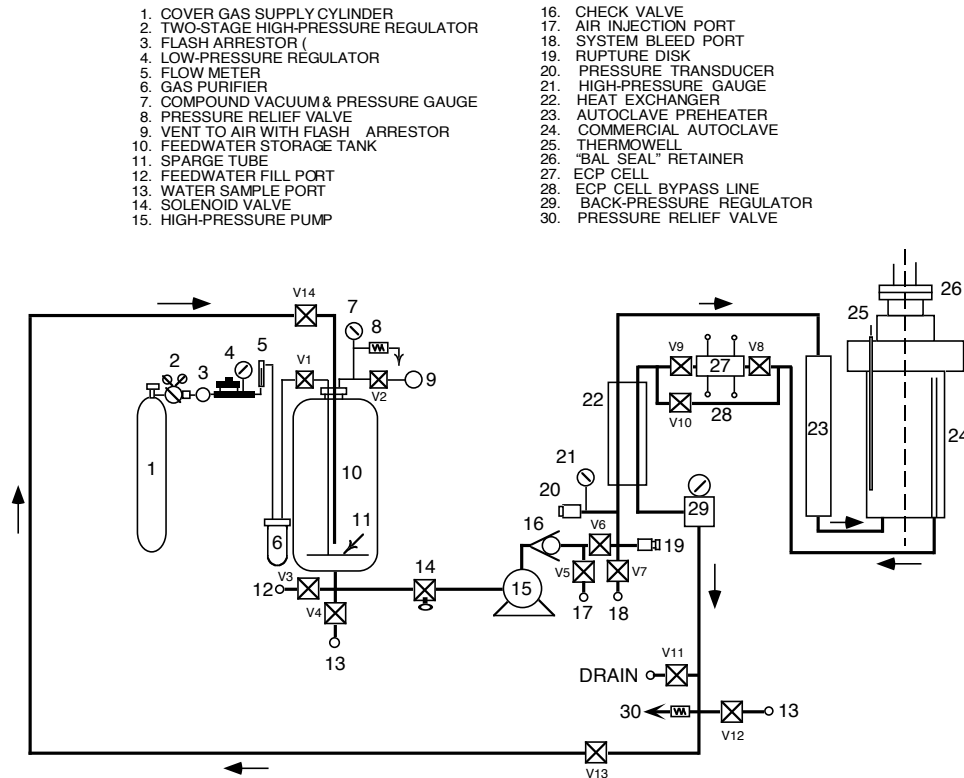


Figure 6. Schematic diagram of the recirculating autoclave system used for crack growth rate tests.

once-through mode, the return line is connected to the drain. During recirculation the ECP cell in the return line from the autoclave to the feedwater supply tank is bypassed. The 5.7-liter Type 316 stainless steel autoclave has a 175-mm (6.875-in.) OD and is rated for a working pressure of 5050 psig (35 MPa) at 343°C (650°F). The system uses Types 316 or 304 stainless steel (SS) tubing. Water is circulated at relatively low flow rates, i.e., 5–15 mL/min.

The feedwater storage tank, manufactured by Filpaco Industries, has 130-L capacity and is constructed of either Type 304 or 316 SS. The tank is designed for vacuum and over-pressure to 60 psig (414 kPa). The storage tank has a hydrogen cover gas to maintain a desired dissolved hydrogen concentration in the water.

The simulated PWR feedwater contains less than 10 ppb DO, 2 ppm Li, 1000 ppm B, and ≈ 2 ppm dissolved hydrogen ($\approx 23 \text{ cm}^3/\text{kg}$). It is prepared from the laboratory supplies of deionized water by first passing this water through a local filtration system that includes a carbon filter, an Organex-Q filter, two ion exchangers, and a 0.2-mm capsule filter. The DO in the deionized water is reduced to <10 ppb by bubbling/sparging a mixture of $\text{N}_2 + 5\% \text{ H}_2$ through the water. To speed deoxygenation, a vacuum may be applied to the feedwater tank at the vent port (item 9). The PWR water is prepared by dissolving boric acid and lithium hydroxide in 20 L of deionized water before adding the solution to the supply tank. The hydrogen gas pressure in the feedwater tank is maintained at 34 kPa. The dissolved hydrogen in water is calculated from the tank hydrogen pressure and temperature.

Water samples are taken periodically to measure pH, resistivity, and DO concentration both upstream and downstream from the autoclave. An Orbisphere meter and CHEMetrics™ ampoules are used to measure the DO concentrations in the supply and effluent water. The redox and open-circuit corrosion potentials are monitored at the autoclave outlet by measuring the ECPs of platinum and an Alloy 600 electrode, respectively, against a 0.1 M KCl/AgCl/Ag external (cold) reference electrode. The measured ECPs, $E(\text{meas})$ (mV), were converted to the standard hydrogen electrode (SHE) scale, $E(\text{SHE})$ (mV), by the polynomial expression²⁹

$$E(\text{SHE}) = E(\text{meas}) + 286.637 - 1.0032(\Delta T) + 1.7447 \times 10^{-4}(\Delta T)^2 - 3.03004 \times 10^{-6}(\Delta T)^3, \quad (4)$$

where ΔT (°C) is the temperature difference of the salt bridge in a 0.1 M KCl/AgCl/Ag external reference electrode (i.e., the test temperature minus ambient temperature).

2.3 Test Procedure

The CGR tests were conducted in the load-control mode using a triangular, sawtooth, or trapezoidal waveform with load ratio R of 0.3–0.7. The CT specimens were fatigue precracked in the test environment and load ratio $R = 0.3$, frequency ≈ 1 Hz, and maximum stress intensity factor K_{max} of 20–25 $\text{MPa}\cdot\text{m}^{1/2}$. After ≈ 0.5 -mm extension, R was increased incrementally to 0.7, and the loading waveform changed to a slow/fast sawtooth with rise times of 30–1000 s. The SCC growth rates were determined using a trapezoidal waveform with $R = 0.5$ or 0.7, 12–1000 s rise time, 3600-s hold period at peak, and 12-s unload time. This loading sequence is considered to result in reproducible CGRs.³⁰ During individual test periods, K_{max} was maintained approximately constant by periodic load shedding (less than 2% decrease in load at any given time).

Crack extensions were monitored by the reversing DC potential difference method. The current leads were attached to the holes on the top and bottom surfaces of the specimen (Fig. 1), and potential leads were welded on the front face of the specimen across the machined notch but on diagonal ends. Also, to compensate for the effects of changes in resistivity of the material with time, an Alloy 600

internal reference bar was installed near the test specimen. The CT specimen and reference bar were connected in series, and the DC potential across the specimen as well as the reference bar was monitored continuously during the test. The results for the reference bar were used to normalize potential drop measurements for the CT test specimen.

Under cyclic loading, the CGR (m/s) can be expressed as the superposition of the rate in air (mechanical fatigue) and the rates due to corrosion fatigue (CF) and stress corrosion cracking (SCC), given as

$$\dot{a}_{env} = \dot{a}_{air} + \dot{a}_{cf} + \dot{a}_{sc} \quad (5)$$

During crack growth tests in high-temperature water, environmental enhancement of CGRs does not occur from the start of the test. Under more rapid cyclic loading, the crack growth is dominated by mechanical fatigue. The CGRs during precracking and initial periods of cyclic loading were primarily due to mechanical fatigue. In general, environmental enhancement is typically observed under loading conditions that would lead to CGRs between 10^{-10} and 10^{-9} m/s in air. The stress intensity factor range ΔK was calculated as follows:

$$\Delta K = \frac{\Delta P}{(B B_N W)^{1/2}} \frac{\left(2 + \frac{a}{W}\right)}{\left(1 - \frac{a}{W}\right)^{3/2}} f\left(\frac{a}{W}\right) \quad (6)$$

$$\Delta P = P_{max} - P_{min} \quad \text{for } R > 0 \quad (7)$$

$$f\left(\frac{a}{W}\right) = 0.886 + 4.64\left(\frac{a}{W}\right) - 13.32\left(\frac{a}{W}\right)^2 + 14.72\left(\frac{a}{W}\right)^3 - 5.6\left(\frac{a}{W}\right)^4, \quad (8)$$

where P_{max} and P_{min} are maximum and minimum applied load, a is crack length, W is the specimen width, and effective thickness $B_{eff} = (B B_N)^{0.5}$. The applied K for the tests was in accordance with the specimen size criteria of ASTM E 1681 and E 647. These criteria are intended to ensure applicability and transferability of the cracking behavior of a component or specimen of a given thickness under a specific loading condition to a crack associated with a different geometry, thickness, and loading condition. The K /size criteria require that the plastic zone at the tip of a crack is small relative to the specimen geometry. For constant load tests, ASTM E 1681 requires that

$$B_{eff} \text{ and } (W - a) \geq 2.5 (K/\sigma_{ys})^2, \quad (9)$$

and for cyclic loading ASTM 647 requires that

$$(W - a) \geq (4/\pi) (K/\sigma_{ys})^2, \quad (10)$$

where K is the applied stress intensity factor, and σ_{ys} is the yield stress of the material. In high-temperature water, because the primary mechanism for crack growth during continuous cycling is not mechanical fatigue, Eq. 9 is probably the more appropriate criterion, but Eq. 10 may give acceptable

results. For high-strain hardening materials, i.e., materials with an ultimate-to-yield stress ratio ($\sigma_{\text{ult}}/\sigma_{\text{ys}} \geq 1.3$), both criteria allow the use of the flow stress defined as $\sigma_f = (\sigma_{\text{ult}} + \sigma_{\text{ys}})/2$ rather than the yield stress.

After the test the specimen was fractured in liquid nitrogen, and the fracture surfaces were examined by optical or electron microscopy to measure the final crack length using the 9/8 averaging technique; that is, the two near-surface measurements were averaged, and the resultant value was averaged with the remaining seven measurements. The number of measurements was increased for irregular crack fronts.

